The seismic view on sediment laden ephemeral flows – modelling of ground motion data for fluid and bedload dynamics in the Arroyo de los Piños

Michael Dietze, Dr, GFZ Potsdam, Potsdam, Germany, mdietze@gfz-potsdam.de
Florent Gimbert, Dr, University of Grenoble Alpes, CNRS, IRD, Institut des Géosciences de l'Environnement (IGE), Grenoble, France, florent.gimbert@univ-grenoble-alpes.fr
Jens M. Turowski, Dr, GFZ Potsdam, Potsdam, Germany, turowski@gfz-potsdam.de
Kyle A. Stark, New Mexico Institute of Mining and Technology, Socorro, NM, kyle.stark@student.nmt.edu
Daniel Cadol, New Mexico Institute of Mining and Technology, Socorro, NM, daniel.cadol@nmt.edu
Jonathan B. Laronne, Dr, Ben Gurion University of the Negev, Beer Sheva, Israel, john@bgu.ac.il

Abstract

Ephemeral streams prone to sediment laden flash floods are key to understand the modes of long term landscape evolution in semi-arid areas, pose a significant hazard to infrastructure and people and are requisite to model the stability of main stem rivers to which they deliver sediment. Key parameters of fluid and bedload dynamics are difficult to measure directly during events unless an extensive measurement infrastructure is installed in the channel. Even then, bedload samplers and pressure transducers provide spatially localised and temporally discrete data that require interpolation to gain representative information about a flash flood event.

Seismometers are potentially valuable alternatives to in-stream devices. Installed at the stream bank, they are safe from damage, continuously record high resolution data, incorporate the average behaviour of a given footprint, and record proxy signals of a series of key parameters. In order to develop these sensors as established devices for monitoring bedload transporting flows, we need to understand what they tell us by unmixing the superimposed signals of the parameters of interest. This requires comparison of data generated by seismic sensors with independent records of established devices.

In this study we exploit the excellent infrastructure of the newly activated Arroyo de los Piños sediment research facility. We make use of seismic signals of a large flash flood event recorded by a broadband seismometer station. We model the seismic spectra due to bedload and flowing water, explicitly taking into account input parameter uncertainty, and compare the results with independent measurements.

Introduction

Understanding the boundary conditions and operational modes of ephemeral streams is essential from a process geomorphology and long term landscape evolution perspective. Ephemeral streams are specifically prone to flash floods, rapidly occurring inundations due to heavy rain. Under such rapid and massive flood conditions, the stream mobilises very high

amounts of bedload (Reid & Laronne, 1995). These flow and transport mechanisms are important to better understand the geomorphic effects of such systems but also to estimate and mitigate effects on infrastructure.

Accordingly, there has been significant effort in collecting instrumental data on key parameters inherent to flow conditions and the boundary conditions determining the dynamics of flash flood events. Classic approaches involve the construction of massive concrete supported infrastructure inside the stream bed. This is necessary to maintain operation under the harsh conditions during events. Typical in-stream instrumentation to constrain flow conditions include pressure gauges, temperature sensors, and turbidity sensors. Bedload dynamics are monitored with time resolving slot samplers and acoustic sensors such as hydrophones and plate geophones (e.g., Cohen & Laronne, 2005; Rickenmann et al., 2014).

Most of these sensors, delivering direct and indirect data on the target parameters, provide point measurements or can at best be regarded as cross sectional lines of sensors. Furthermore, the in stream instrumentation approach requires careful planning of suitable deployment sites as a massive investment is involved and a characteristic reach needs to be identified. The maintenance effort is significant.

In recent years, a valuable alternative and complementary approach has gained increasing attention: out-of-stream instrumentation with seismic sensors (Burtin et al., 2008; Barrierére et al., 2015; Schmandt et al., 2017). Such sensors are installed at a safe distance to the stream and record the ground motion due to stream dynamics, along with a series of further seismic sources. Modern seismic stations can be deployed easily under rugged conditions and are able to operate autonomously for months without maintenance; some systems are even capable of near real time data telemetry. They provide continuous high resolution (> 200 Hz) time series that carry information averaging over a given footprint of tens to thousands of metres. Thus, seismic stations may provide near real time high quality proxy data of key parameters otherwise hard to obtain.

Physical models were suggested to predict the seismic frequency spectra caused by earth surface dynamics, such as turbulent fluid flow (Gimbert et al., 2014) and river bedload transport (Tsai et al., 2012; Gimbert et al., 2018). In order to make appropriate use of such models, it is important to explore robust ways to apply them inversely, i.e., to invert flow bedload and flux properties from the measured seismic data.

We make use of the excellent infrastructure of the Arroyo de los Piños sediment research facility (Varyu et al., –this issue). We explore to which extent physically based model results (Tsai et al., 2012; Gimbert et al., 2018) are consistent with seismic signals recorded next to the instrumented stream.

Study site

The United States Bureau of Reclamation identified the Arroyo de los Piños as a prime candidate to improve Rio Grande sediment dynamics modeling. Work began on a world-class sediment monitoring station on the Piños with construction being completed in early 2018. The catchment size is 32 km^2; as tributary of the Rio Grande, the Piños is typical of many systems found in the southwestern United States. Flash floods carry sediment directly into the Rio Grande causing a localized influx at the point of confluence. The Piños is located at the northern

extent of the Chihuahuan Desert; characterized by violent monsoonal storms during the summer months. Most of the runoff observed in the Piños to date comes from these monsoonal storms.

Materials and methods

Instrumentation and seismic setup

A 9.1 m wide cross section of the Arroyo de los Piños has been turned into a sediment dynamics research facility by installing a concrete lined sill. Into its concrete floor a series of in stream sensors have been embedded. For details see Varyu et al. (this issue).

In addition, a Nanometrics Trillium Compact TC120s broadband seismometer has been installed on the bank, 6 m away from the stream margin. The sensor was inserted into a 50 cm deep hand dug pit, oriented to the North and levelled horizontally, mantled with sand and the pit was closed again. The ground motion signals are recorded by a Nanometrics Centaur data logger, operating at a recording frequency of 1000 Hz, with a dynamic range of 10 Vpp (gain = 4).

Data analysis

The analysis focuses on the largest flash flood event in 2018 (Figures 1, 2). The measured seismic data were prepared and analysed with the R package 'eseis' (Dietze, 2018). The continuous time series were imported for the flood event duration, and their means and linear trends were removed. The instrument response was removed, also accounting for the dynamic range of the logger, and the data was high pass filtered with a lower cut-off frequency of 1 Hz to remove the ocean signal content. Spectrograms were calculated from the tapered time series (taper size 0.5 % of the total time series length) using the sub window averaging approach (Welch, 1967) on periodogram-based spectra, each calculated from 80 % overlapping data snippets with window sizes of 40 and 20 s, respectively.

Seismic models

During flash flood events, the seismic signal at the Arroyo de los Piños facility is expected to be dominated by the effects of turbulent fluid flow and/or the seismic wave scape due to particles impacting the bed. Secondary effects may be caused by rainfall at the site, but more severely by road traffic and people walking past the sensor. A further source of seismic signals can be other rivers, such as the Rio Grande, some 250 m westwards. During this event operators arrived at the site too late to cross the river toward the station; hence, noise due to persons or vehicles was probably absent.

To explore the potential effect of fluid flow and bedload transport, we calculated seismic spectra based on the models of Gimbert et al. (2014) and Tsai et al. (2012), respectively. Both models are physically based representations of first order processes that cause ground motion as recorded by seismic stations. The two models are part of the R package 'eseis', rewritten from the original publications and validated against the corresponding Matlab script outputs. The models require a range of parameters (Table 1) to be set or estimated, in order to account for properties of the fluid, the transported sediment particles, the bed characteristics and the properties of the medium through which the seismic waves travel toward the sensor.

Since several of these parameters remain unknown or can only be provided with an associated uncertainty, we have to account for different model realisations, i.e., propagating the input parameter uncertainties through the modelling process into the model output. For such highly complex, non-linear and partly approximating models, there is no straightforward analytic approach to uncertainty implementation. Thus, we use a Monte Carlo approach (cf. Dietze, 2018). We run both models multiple times (10,000 in our case), each time with slightly different parameter values. The values are drawn from uniform random distributions. Each model output is stored and the resulting assemblage of data is used to generate average seismic model spectra and confidence intervals (quartile ranges). The spectra were calculated for different potential stages of the flood and bedload fluxes. Table 1 summarizes the model parameters along with their ranges of possible values. The parameter ranges are based on empirical field data, results of studies under comparable landscape configurations, and best knowledge estimates, as indicated in Table 1.

Table 1. Parameters and estimated uncertainty ranges for physically based models to predict the seismic spectra due to turbulent water flow and bedload sediment transport (s.d. means dimensionless).

Paramater (unit)	Symbol	Value range/fixed	Justification
D_{50} bedload grain diameter (m)	d_s	0.007–0.009	field sample measurements
Grain diameter standard deviation (log m)	s_s	0.5–0.9	field sample measurements
Bedload sediment flux (m^2/s)	q_s	see figure 4	observatory data result
Sediment density (kg/m^3)	r_s	2600–2700	average rock density
Fluid density (kg/m^3)	r_w	1000–1200	density of water with suspended load
Water depth (m)	h_w	see figure 4	observatory data
Channel width (m)	w_w	9–10	observatory data
Channel slope (radians)	a_w	0.016–0.020	observatory data
Distance river to station (m)	r_0	6	observatory data
Reference frequency (Hz)	f_0	1	Tsai et al. (2012), Gimbert et al. (2014)
Material quality factor at f_0 (s.d.)	q_0	10–20	Tsai et al. (2012), Gimbert et al. (2014)
Rayleigh wave phase velocity at f_0	v_0	400–600	estimate based on Dietze (2018)
Variation coefficient for v_0	p_0	0.6–0.7	Tsai et al. (2012), Gimbert et al. (2014)
Q increase with frequency (s.d.)	e_0	0.0–0.2	Tsai et al. (2012), Gimbert et al. (2014)
Greens function displacement amplitude coefficients (s.d.)	n_0	0.6–0.8, 0.8–0.9	Lagarde et al. (unpublished)

Results

Empirical data

The largest sediment laden flash flood event of 2018 was caused by 30 mm precipitation in the upstream section of the catchment around 10 am on 26 July, preceded and succeeded by smaller precipitation events. Moving southward, the main storm also caused precipitation affecting adjacent catchments and the trunk stream, the Rio Grande. Flow was recorded at the monitoring station over 5.5 hours (22:06–03:30 local time, 04:06–9:30 UTC time – UTC time unit used hereafter). Within one hour the stage rose to peak at 1.61 m and then receded during 4.5 hours (Figure 1). With the onset of flow, the bedload samplers started filling, most pronounced in the left and central device. These filled within a few minutes while the right sampler collected bedload for a few more minutes. Thus, data from these devices cannot be used for the entire flood event and have been truncated in figure 1. However, the pipe microphones, collecting surrogate data of bedload particle impacts were in operation throughout the event. The two sensors show significantly differing time series.

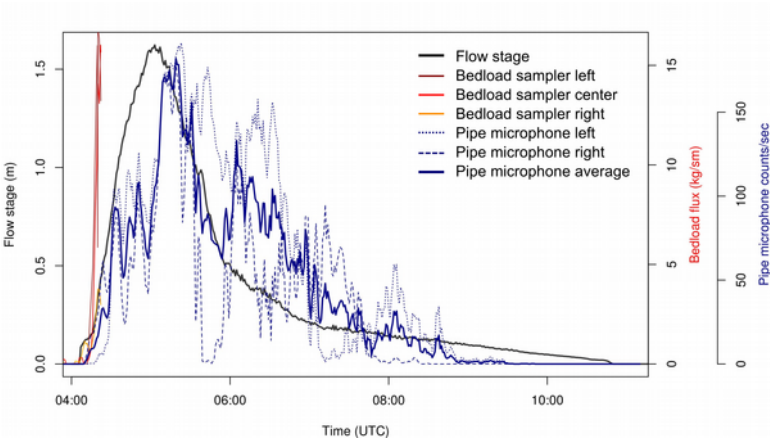

Figure 1. Sensor time series of the sediment laden flash flood in the Arroyo de los Piños. The hydrograph (black line) shows a rapid stage rise just after 4 am (UTC time) with recession lasting until 10 am on July 27 2018. Bedload flux was massive enough to fill all three Reid type basket samplers. The pipe microphone count data (left sensor dotted line, right sensor dashed line, average solid bold line), show bedload movement for about five hours.

The seismic perspective on this flash flood event (Figure 2a) shows the preceding conditions and the seismic background signals superimposed on the actual target processes. The rain events appear as vertical bands due to their broad band frequency character (Dietze et al., 2017). A 2-8 Hz frequency band is continuously present (horizontal green line in Figure 2a). The most prominent feature in the spectrogram is the flood event (Figure 2b). Its onset at 4:10 am is recorded as a sudden increase in seismic energy across almost the entire frequency space, followed by the emergence of another, even more energetic pulse around 4:20 am. Most seismic energy is carried by frequencies in the range 4–12 Hz with a gliding upward trend as the flood progresses.

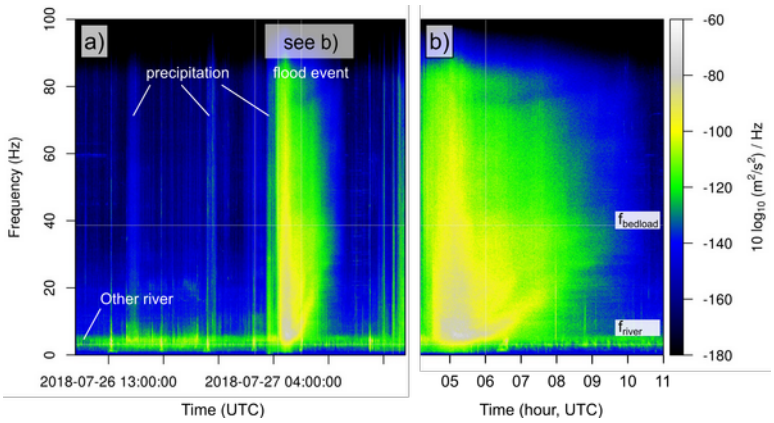

Figure 2. Seismic spectrograms (time-frequency plots) of the investigated flash flood event. a) overview including preceding phase with multiple rain events (vertical broad frequency bands) and the continuous 2-8 Hz frequency band signal generated by another continuous source (horizontal band). b) close-up of the flood event, dominated by frequencies between 4 and 30 Hz. The white bands in b) denote frequency ranges used to generate time series of seismic activity in Figure 3, assumed to be dominated by turbulent flow in the Arroyo de los Piños (f_{river}) and bedload impacts ($f_{bedload}$).

Following suggestions from the literature (e.g., Gimbert et al., 2014; Cook et al., 2018) we extract average seismic power time series from the spectral data in the two discrete frequency bands 5–8 Hz and 35–40 Hz, which supposedly are characteristic of river turbulence and bedload impacts, respectively. The resulting surrogate time series (Figure 3) show the general co-evolution of the two supposed sources of seismic energy. However, they also show that the

portion of signal caused by bedload impact behaves differently during recession than the fluvial signal source. Both time series are similar to the evolution of the independently measured data sets. The hydrograph and the 5–8 Hz band both rise from the onset of the flood at 4:06 am, peak around 5 am and fall to background values by 10 am. However, the peak of the seismic time series is broader and the falling limb shows another, secondary maximum between 6:10 and 7:00 am, which is not visible in the pressure gauge data. Seismic power characteristic for bedload flux appears to rise steeper and less uniform than the other seismic time series before it also peaks around 5 am. Overall, the data shows greater differences from the averaged pipe microphone time series, most notable it does not show the plateau-like evolution in the rising part.

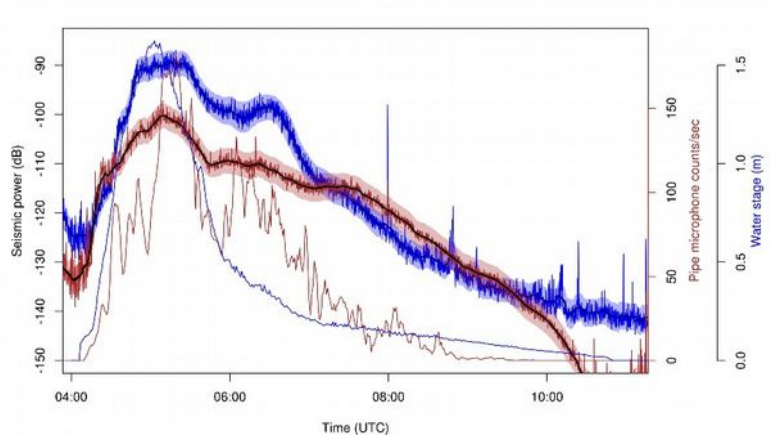

Figure 3. Seismic power time series, supposed to be characteristic for turbulent fluid flow (5–8 Hz, blue lines) and bedload particle impacts (35–40 Hz, brown lines), corresponding to the annotations in Figure 2b. The plot shows the raw seismic data (solid thin lines) and their one standard deviation ranges (polygons) as well as 200 sample wide running averages (thick lines) in dB, i.e., $10 \cdot \log_{10}(m^2/s^2/Hz^2)$. The independently measured time series of water stage (thin blue line) and bedload impact related average pipe microphone (thin brown line) are given for comparison.

Seismic models

Turbulence signatures (after Gimbert et al., 2014) were calculated for flow depths from 0.05 to 2 m (Figure 4a), with relevant model parameters being allowed to range freely within meaningful limits (cf. Table 1). This range in depth covers most of the independently measured values (0–1.61 m) and the corresponding spectra span the majority of the energy levels of spectra measured by the broadband station (grey curves in Figure 4a). However, the shape of the modelled turbulence spectra is obviously different from the empirical one; most prominently below 20 Hz and above 60 Hz.

Bedload models (after Tsai et al., 2012) cover seven orders of magnitude, from 0.1 g/sm to 100 kg/sm. The lower value was set after exploring which flux best matches the lowest empirical spectrum. The highest value was set based on scaling the Reid type sampler values by the pipe microphone data (about 60 kg/sm). Here as well, the resulting spectra represent the range of the empirical data (grey curves in Figure 4b) but deviate significantly from those, predominantly, below 40 Hz.

Both model spectra overlap significantly and have their highest values in frequency bands different from the bands denoted in Figure 2 (5–8 Hz and 35–40 Hz). This underlines the ambiguities with separating the two sources of seismic signals by simply isolating these two

frequency bands. The overlap is caused not only by the range of individual spectra as a result of input parameter uncertainty and scatter, but also by the overall shape of the two model outputs.

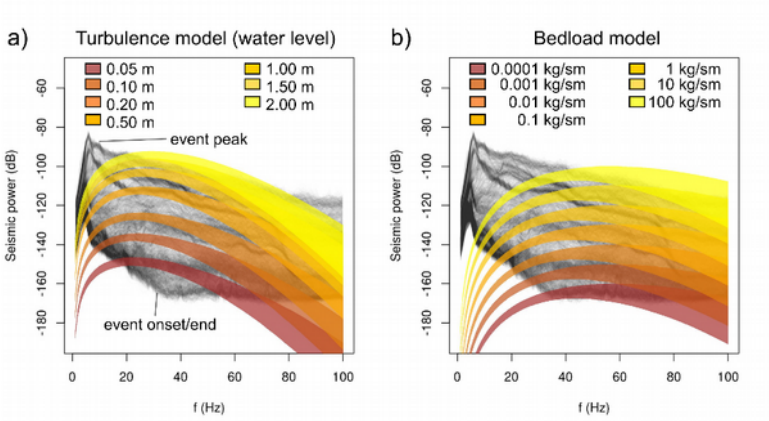

Figure 4. Modelled seismic spectra caused by a) water turbulence and b) bedload transport. Shaded polygon area depicts inter quartile range of model solutions due to input parameter uncertainty. Grey curves in the background depict empirical spectra as measured by the broadband seismometer over the duration of the flash flood (i.e., corresponding to the vertical dimension of the spectrogram in figure 2).

Discussion

Clearly, there is a relation between the seismic record and fluvial dynamics. But this relation is far from straightforward. The temporal evolution of the seismic frequency bands, supposed to represent turbulence and bedload transport, deviates significantly from independently measured proxy data. Deviation may at least for the bedload proxy data be due to cross-sectional differing pipe microphone impact rates (dashed vs. dotted lines in Figure 1), caused by spatially non-uniform particle flux or cover and dampening effects. This highlights the need for a spatially averaging technique if the goal is to infer the general flow and flux characteristics, not only in a cross-sectional dimension but also along stream.

During this significant flood, two of the three Reid type basket samplers filled by a small fraction of the transported bedload. Furthermore, the pit samplers also show a spatially non-uniform evolution. These results also argue for the need of an additional, continuous and spatially averaging monitoring technique to better constrain the general event characteristics.

The seismic data indicate convolution of at least three sources of seismic signals. Although the Rio Grande would be able to cause seismic signals in the 2–8 Hz range (Cook et al., 2018), which is clearly visible before and after the flood event, it is unlikely to be the cause of the low frequency peak in the spectra as it cannot reach beyond -160 dB even under enormous flow conditions (model results not shown, based on 250 m distance to station, 80 m width, 3 m depth, coarse sand D_{50}). Thus, it is likely that other tributary channels or continuously operating seismic sources are responsible for the contamination of the data in this frequency band. The 5–8 Hz band as proxy for channel flow activity starts at a higher energy level than after the flood. This is most likely due to energy leaking from the 2–8 Hz seismic source into the 5–8 Hz frequency band. This tendency is visible in Figure 2a, where the persistent frequency band is active also hours before and after the flood event.

The observed spectra (Figure 4, grey background lines) can be explained in major parts (i.e., frequencies > 20 Hz) by a combination of the two seismic models (Tsai et al., 2012; Gimbert et

al., 2014). However, the dominant low frequency part (2–8 Hz) is not reproduced by any of the models. It may be related to local effects, such as the concrete reinforced cross section, resonating in its characteristic frequency. More investigations are needed to explore this effect, either by modelling the characteristic frequency of such a concrete body or by conducting dedicated seismic sensing of this structure. Likewise, the low power spectra, before the flood starts and just after it ended (i.e., low power spectra lines in Figure 4), only follow the flat -160 dB shape of typical “environmental noise” spectra above 40 Hz, while seismic power steadily rises below this frequency.

The convolution of channel flow turbulence and bedload flux signal is obvious when considering the Monte Carlo based seismic spectra models (Figure 4). While the turbulence spectra match the frequency range 20–60 Hz and the bedload spectra better describe the frequency range 60–100 Hz, both estimates overlap. Except for the extreme periods in water stage (1.61 m) and bedload flux (perhaps 20 kg/sm) – for which there is indeed agreement of empirical and modelled spectra – the number of potential combinations of similar likely spectra due to the two sources is high. This makes simple frequency band time series as proxies for water stage and bedload flux questionable, at least under the current setting of this observatory.

Accordingly, a more robust approach should explicitly account for the combined effect of at least two different seismic sources, thereby taking into account a wide range of frequencies along with the shape of the modelled spectra. Furthermore, uncertainty in the model parameter space should feed into the robust approach to develop a realistic estimate not only of the most likely values for key flood event metrics, but also their uncertainties. Thus, a Monte Carlo based inversion of physically based seismic models appears a prosperous approach to this problem.

Conclusion

In this ongoing study we used a seismic instrument as a high resolution, non-invasive sensor to continuously survey the spatially averaged characteristics of a sediment laden flash flood event at safe distance to the channel and its devastating effects. We compared the seismic ground motion data with other, independently constrained flood proxy data, and explored to which extent existing physically based seismic model results agree with the empirical data.

The spectral information in the seismic data (figure 2) show a distinct evolution of the signals contained in different frequency bands (figure 3), which is in general consistent with expectations from theory. While it would be appealing to extract key flood parameters by conveniently deploying a state of the art seismic station, there are several shortcomings adherent to this approach. The seismic data are by no means straightforward to interpret. The spectra emitted by at least three temporally distinct sources overlap significantly, whereby the source of a low frequency (2–8 Hz) signal is not yet resolved, but may perhaps be related to the characteristic frequency of the concrete structure of the observatory. Furthermore, the seismic station is subject to the influence of further seismic sources such as wind, rain, anthropogenic activity (though not in this particular case) and other river systems. Existing physically based model predictions fall well into the range of empirically determined data but overlap to a significant degree. Accordingly, it is vital to develop a manner to handle this mixed nature of the signals we record.

In addition, and in the light of the expected lifetime of the observatory, it might be valuable to reconfigure the seismic station components. The seismic data show that there is no need to work with broadband instrument data, as most of the signals of interest are > 1 Hz, whereas the

currently used sensor is ideal for frequencies between 0.008 and 200 Hz. Likewise, none of the models is designed for other than the vertical component data. Thus, it would be an option to replace the one three-component broadband sensor by three single-component geophones. These can be arranged in a triangular geometry with two sensors along stream and one sensor ca. 40–70 m away. Such a setup would allow for more profound insight into streamwise changes in hydraulic and sediment transport dynamics, but also allow a more robust inversion by adding a further data set at another distance to the channel, with other expected spectral properties to include to the inversion approach.

Acknowledgements

The authors are thankful to Sophie Lagarde for the tedious work of translating the seismic models to R.

References

Barrière, J., Oth, A., Hostache, R. and Krein, A. 2015. “Bed load transport monitoring using seismic observations in a low-gradient rural gravel bed stream,” Geophys. Res. Lett., 42, 2294–2301, doi:10.1002/2015GL063630.

Burtin, A., Bollinger, L., Vergne, J., Cattin, R. and Nábělek, J.L. 2008. “Spectral analysis of seismic noise induced by rivers: A new tool to monitor spatiotemporal changes in stream hydrodynamics,” J. Geophys. Res., 113, B05301, doi:10.1029/2007JB005034.

Cohen, H., and Laronne, J.B. 2005. “High rates of sediment transport by flashfloods in the Southern Judean Desert, Israel”, Hydrological Processes, 19, 1687-1702, doi: 10.1002/hyp.5630.

Cook, K., Andermann, C., Gimbert, F., Raj Adhikari, B. and Hovius, N. 2018. “Glacial lake outburst floods as drivers of fluvial erosion in the Himalaya,” Science 362, 6410, 53-57, doi: 10.1126/science.aat4981.

Dietze, M. 2018. “The R package ‘eseis’ – a software toolbox for environmental seismology,” Earth Surf. Dynam., 6, 669-686, doi: 10.5194/esurf-6-669-2018

Dietze, M., Turowski, J.M., Cook, K.L. and Hovius, N. 2017. “Spatiotemporal patterns, triggers and anatomies of seismically detected rockfalls,” Earth Surf. Dynam., 5, 757–779, doi: 10.5194/esurf-5-757-2017.

Gimbert, F., Tsai, V.C. and Lamb, M.P. 2014. “A physical model for seismic noise generation by turbulent flow in rivers,” J. Geophys. Res., 119, 2209–2238, doi: 10.1002/2014JF003201, 2014.

Gimbert, F., Fuller, B. M., Lamb, M. P., Tsai, V. C., and Johnson, J. P. L. 2018. “Particle transport mechanics and induced seismic noise in steep flume experiments with accelerometer-embedded tracers,” *Earth Surf. Process. Landforms*, 44, 219–241, https://doi.org/10.1002/esp.4495.

Reid, I. and Laronne, J.B. 1995. “Bedload sediment transport in an ephemeral stream and a comparison with seasonal and perennial counterparts”, Water Resources Research, 31 (3), 773-781, doi:10.1029/94WR02233.

Rickenmann, D., Turowski, J.M., Fritschi, B., Wyss, C., Laronne, J.B., Barzilai, R., Reid, I., Kreisler, A., Aigner, J., Seitz, H. and Habersack, H. 2014. “Bedload transport measurements with impact plate geophones: comparison of sensor calibration at different gravel-bed streams“, Earth Surface Processes and Landforms 39, 928-942. DOI:10.1002/esp.3499

Schmandt, B., Gaeuman, D., Stewart, R., Hansen, S.M., Tsai, V.C. and Smith, J. 2017. “Seismic array constraints on reach-scale bedload transport”. Geology.

Tsai, V., Minchew, B., Lamb, M.P. and Ampuero, J.-P. 2012. “A physical model for seismic noise generation from sediment transport in rivers,” Geophys. Res. Lett., 39, L02404, doi: 10.1029/2011GL050255.

Welch, P.D. 1967. “The use of fast Fourier transform for the estimation of power spectra: A method based on time averaging over short, modified periodograms,” IEEE T. Audio. Speech., 15, 70–73.